

One Step ATRP Initiator Immobilization on Surfaces Leading to Gradient-Grafted Polymer Brushes

Bryan R. Coad,^{*,†} Katie E. Styan,[‡] and Laurence Meagher[‡]

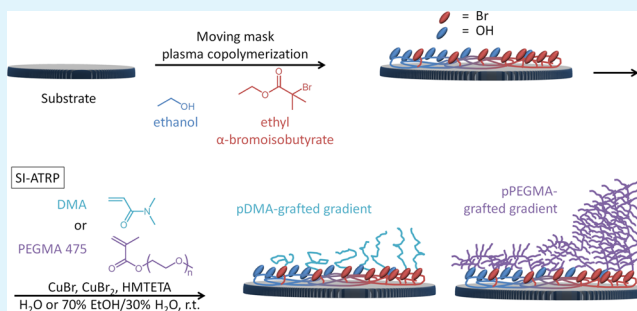
[†]Mawson Institute, University of South Australia, Mawson Lakes SA 5095, Australia

[‡]CSIRO Materials and Science Engineering, Clayton VIC, 3163, Australia

S Supporting Information

ABSTRACT: A method is described that allows potentially any surface to be functionalized covalently with atom transfer radical polymerization (ATRP) initiators derived from ethyl-2-bromoisobutyl bromide in a single step. In addition, the initiator surface density was variable and tunable such that the thickness of polymer chain grafted from the surface varied greatly on the surfaces providing examples, across the surface of a substrate, of increased chain stretching due to the entropic nature of crowded polymer chains leading toward polymer brushes. An initiator gradient of increasing surface density was deposited by plasma copolymerization of an ATRP initiator (ethyl 2-bromoisobutyrate) and a non-ATRP reactive diluent molecule (ethanol). The deposited plasma polymer retained its chemical ability to surface-initiate polymerization reactions as exemplified by *N,N'*-dimethyl acrylamide and poly(ethylene glycol) methyl ether methacrylate polymerizations, illustrating linear and bottle-brush-like chains, respectively. A large variation in graft thickness was observed from the low to high chain-density side suggesting that chains were forced to stretch away from the surface interface—a consequence of entropic effects resulting from increased surface crowding. The *tert*-butyl bromide group of ethyl 2-bromoisobutyrate is a commonly used initiator in ATRP, so a method for covalent linkage to any substrate in a single step desirably simplifies the multistep surface activation procedures currently used.

KEYWORDS: surface-initiated atom transfer radical polymerization, gradient, plasma polymerization, tertiary butyl bromide initiator, substrate independent



INTRODUCTION

Surface-initiated atom transfer radical polymerization (SI-ATRP) is an important method for preparing surfaces with closely packed, terminally attached polymer chains—so-called polymer brushes—with far reaching applications in biomaterials, sensing, separation science, to name a few.^{1–6} The conformations that end-grafted polymer chains adopt is dictated by choice of monomer, the degree of polymerization, the enthalpy of interaction with solvent, and the system entropy restricted by chain–chain interactions with near neighbors.⁷ In practice, this last factor is dictated predominantly by the distance separating neighboring chains,⁸ which for a given SI-ATRP system is a function of the surface density of initiating sites (initiators). Since increased surface grafting density is considered a key determinant to providing an entropic driving force allowing brush conformation, considerable effort has been expended in controlling the initiator surface density.^{3,9,10} Surfaces with steadily increasing surface densities of ATRP initiators (referred to as gradient initiator surfaces) are potentially useful because they exemplify, on a single surface, the influence that a continual variation in grafting density exerts on the physical properties manifest in the grafted layer.^{11–14}

There exist a number of ways to functionalize surfaces with gradients of ATRP initiators. They are based mainly on well-known paired linking chemistries that depend upon established chemical affinities of silanes for silicon^{15,16} or thiols for gold surfaces.¹⁷

Plasma polymerization, sometimes referred to as plasma enhanced chemical vapor deposition, is an established surface functionalization technique allowing many common chemical functional groups (aldehyde, hydroxyl, amine, carboxylic acid, hydrocarbon for example) to be covalently attached to surfaces in a largely substrate independent fashion.^{18–21} Deposition of a plasma polymer onto a substrate provides a way to incorporate new functional groups that can be derivatized, providing ATRP initiators which then allow covalent grafting polymers from many surfaces.^{22,23} For polymeric surfaces that often lack appropriate chemical functionalities for derivitization, this two-step process of plasma polymerization and chemical transformation into ATRP initiators provides a pathway allowing grafting from surfaces by SI-ATRP.^{24–26} Recently, we described

Received: February 19, 2014

Accepted: April 30, 2014

Published: April 30, 2014

a method for preparing a gradient of polymer brushes using this two-step methodology.²⁷

A simpler, one step covalent attachment of potential ATRP initiators to any surface would be of great value to the field of surface grafting. This requires the chemical precursor to be brought into the vapor phase, electrically excited into a plasma that generates charged fragments, radicals, and neutral species, which are subsequently deposited onto the substrate material. Successful deposition of compounds that would function as ATRP-active materials would have to survive this process with the halogen-carbon bond intact and of a chemical environment that provides radical stabilization during initiation in the atom transfer processes. Furthermore, the plasma-deposited material should remain firmly attached to the substrate preventing delamination of the initiator layer throughout the grafting process, even under the increased surface pressures exerted by densely grafted polymer brushes.²⁸ In the research group of Badyal, Teare et al. have used pulsed plasma polymerization of 2-bromoethyl acrylate and vinyl benzyl chloride to form plasma polymers from which polymer brushes were grafted using SI-ATRP.²⁹ There are further examples of the utility of plasma polymerization of vinyl benzyl chloride from Badyal's research group.^{30–33} Here, plasma conditions required rapidly turning on and off the radiofrequency generator on the order of milliseconds (so-called pulsed plasma polymerization) to improve the incorporation of halogen atoms on the surface. Compounds possessing 2-bromoisobutryl ester groups were some of the first reported ATRP initiators,³⁴ and in general, they have become one of the most popular choices for surface initiated ATRP to form grafted polymer brushes.⁴ Ethyl 2-bromoisobutyrate has a vapor pressure that allows sufficient evaporation under vacuum within a plasma chamber. Thus, with appropriate choice of plasma conditions, it should be possible to generate a plasma polymer from this compound and deposit it onto surfaces. To date, and to the best of our knowledge, there have been no reports so far showing successful deposition of plasma polymers, whether ATRP-active or not, derived from 2-bromoisobutryl esters. A one step method for decorating potentially any surface with ATRP-active isobutryl groups would be highly advantageous and provide a universal grafting solution for many surfaces based on familiar chemistries.

In the present work, we demonstrate successful surface functionalization with ATRP-active 2-bromoisobutryl groups illustrating how, in a single processing step, potentially any surface can be transformed into one capable of SI-ATRP. Our approach also provides a way of modulating the grafting density by varying the ratio of initiating groups to nonreactive diluent groups in the plasma copolymerization. We show that grafting by SI-ATRP of linear and bottle-brush polymers produces gradient grafted layers, which are believed to transition from polymer "mushroom" morphologies to densely grafted polymer "brushes".

MATERIALS AND METHODS

Materials. Water was purified (>18 M Ω cm) by use of either a P.Nix UP 900 purification system (Human Corp. S. Korea), a Millipore Gradient, or Direct-Q 5 ultrapure water system. Ethyl 2-bromoisobutyrate (EBiB, 98%), dimethylacrylamide (DMA, 99%), poly(ethylene glycol) methyl ether methacrylate (PEGMA, $M_n = 475$), 1,1,4,7,10,10-hexamethylenetetramine (HMTETA, 97%), copper(I) bromide (Cu(I), 99.99%), copper(II) bromide (Cu(II), $\geq 99\%$), sodium hydrogen sulphite (NaHSO₃, $\geq 99\%$), and inhibitor-remover were purchased from Sigma-Aldrich. Ethylenediamine-tetraacetic acid

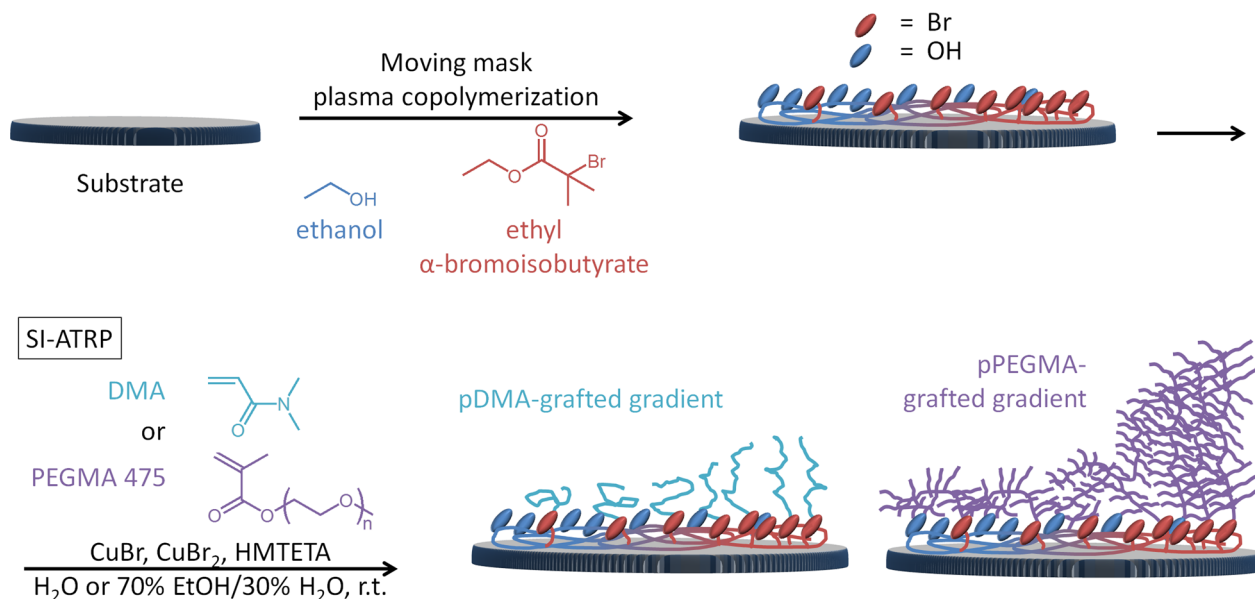
disodium salt (Na₂EDTA, 99.5%) was obtained from BDH, Australia. Ethanol (undenatured 100%, analytical reagent) was purchased from Chem-Supply, Australia. Thermanox polymeric coverslips (13 mm diameter, 0.2 mm thick) were purchased from Thermo Scientific. Thermanox is a solvent resistant, flexible polymeric material made from polyester. Tissue-culture polystyrene (TCPS) MicroWell Plates were obtained from Nalge Nunc International.

Gradient Plasma Polymerization. Gradient copolymerization was performed using a plasma apparatus with a 13.56 MHz radio frequency generator, as previously described.^{27,35–37} A slit mask (1 mm wide) was moved over the Thermanox substrates while simultaneously changing the vapor composition of both EBiB and ethanol using programmed valves. EBiB vapor was introduced at approximately 10 standard cubic centimeters per minute (sccm) and the plasma was ignited at 40 W (as read from the digital power meter readout) as the substrate mask began to move in steps of 0.25 mm every minute. The monomer flask was partially immersed in a hot water bath during polymerization. EBiB vapor was linearly reduced from 10 to 0 sccm as the mask was moved from 3 to 10 mm along the substrate. Concurrently, the ethanol vapor flow rate was linearly increased from 0 to 10 sccm over the same positions and then maintained at 10 sccm from 10 to 14 mm. The anticipated thickness of the initiator plasma copolymer was expected to be approximately 10 nm. Since XPS analysis of films less than 10 nm thick could include ejected photoelectrons from the underlying substrate, for convenience of analysis, substrates were first coated with a homogeneous layer of ethanol plasma polymer (10 sccm, 40 W for 4 min) resulting in an underlayer of ethanol plasma polymer 7.7 nm thick.

Grafting from Gradient ATRP Initiator Plasma Polymer Substrate. DMA and PEGMA were deinhhibited by passage through 2 cm of inhibitor remover resin in a column, and then deoxygenated by bubbling with N₂ for 30 min in a glovebox. Catalyst solution comprising Cu(I) as activating catalyst, Cu(II) as deactivating catalyst and HMTETA as chelating ligand was prepared in solvent (water for DMA and 70 v/v% ethanol in water for PEGMA) and then similarly deoxygenated. Monomer was added to the catalyst solution to give a final monomer concentration of 1 M for PEGMA and 0.5 M for DMA, and a molar ratio of monomer: Cu(I):Cu(II):HMTETA of 20:1:0.2:2 for each. Additional solvent was added to prepare solutions of lower monomer concentration as required. Reaction solutions were mixed and 2 mL immediately applied to each sample independently in wells of a 24-well TCPS plate. The reaction was allowed to proceed in the glovebox at a temperature of about 30 °C on a shaker for 24 h and then was terminated by exposure to air. Coated samples were washed successively with water, 50 mM Na₂EDTA, and 50 mM NaHSO₃ solutions, and then were exhaustively washed with water before being dried under purified nitrogen.

Surface Chemical Characterization. Coated samples were analyzed for their surface chemical compositions using a Kratos Axis Ultra DLD X-ray photoelectron spectrometer (XPS) equipped with a monochromatic Al K α source. Charging of the samples during irradiation was compensated by an internal flood gun. Each sample was analyzed at an emission angle normal to the sample surface. Survey spectra were acquired at 120 eV pass energy and high-resolution C 1s spectra were recorded at 20 eV pass energy. Data were processed with CasaXPS (ver.2.3.16 Pre rel. 1.4, Casa Software Ltd.) with residuals for curve fits minimized with multiple iterations using simplex algorithms. Spectra were corrected for charge compensation effects by offsetting the binding energy relative to the C—C component of the C 1s spectrum, which was set to 285.0 eV. A generalized peak fitting procedure applicable to plasma polymerized organic molecules was used to assign binding energies to photoelectrons.³⁸ C1 was assigned to C—C and C—H, C2 assigned to secondary shifted aliphatic carbons bound to electronegative elements (C—C—X), C3 assigned to ether and alcohol carbons (C—O), C4 to carbonyls (C=O), and C5 to esters (C—O—C=O) and amides (C—N—C=O). In some cases, a small sixth component C6 could be fit. Uncertainties in peak fittings were determined using a Monte Carlo procedure.

Thickness Measurements. Layer thicknesses from gradient samples on Thermanox were determined through the use of a

Scheme 1. One Step, ATRP Initiator Functionalization of Surfaces Using Plasma Co-polymerization^a

^aInitiator gradients produce polymer-grafted surface density gradients after SI-ATRP.

variable-angle spectroscopic ellipsometer (VASE, J.A. Woolam Co. Inc. NE, U.S.A.). Data were acquired at 65°, 70°, and 75° with light wavelengths scanned from 250 to 1100 nm in 10 nm intervals. An autoretarder was used to modulate the polarization of the incoming light beam to five different states before striking the sample, which produces optimal measurement conditions allowing high-accuracy analysis. Samples were prepared by affixing a piece of transparent adhesive tape on the back-side of the sample, as this scatters light reflecting from the back-side of the transparent coverslip and thus reduces interference with reflections from the sample-side. Data were obtained on unfunctionalized coverslips, and a model for refractive index and extinction coefficient for the substrate were established from the best fit to a Cauchy model. Coated samples (initiator and then polymer) were analyzed at positions across the substrate by a programmed translating sample stage. Data at each point were fit to a two layer model for Ψ and Δ composed of an infinitely thick Thermanox substrate (determined above) with Cauchy overlayer. A minimum number of uncorrelated fitting parameters (optical constants in the Cauchy layer) were used to fit both the optical properties of the film and the film thickness. The area of the light beam used for ellipsometry ($\sim 1 \text{ mm}^2$) is on the same order as the length scale of the gradient meaning that for steep gradient samples; there is a potential source of error from sample inhomogeneity. Accuracy was generally improved by the high-accuracy analysis afforded by the autoretarder. For all fits, differences between the obtained data and mathematical model (the mean squared error, M.S.E.) were minimized and larger final M.S.E. values resulted in larger absolute error values. These uncertainties are represented in the data and graphs as error bars. Thicknesses of the SI-ATRP polymer layer only were obtained by subtracting the total layer thickness from the thickness of the underlying plasma polymer.

Note that for convenience XPS and ellipsometry data were measured and are presented beginning at the low-Br containing (i.e., predominantly ethanol) side and continuing toward the high-Br containing (i.e., predominantly EBiB) side in increments of 1 mm by use of an X,Y-micrometer stage, which is opposite to the length scale defined during plasma deposition. The first position, denoted as 1 mm in the data, was estimated.

RESULTS AND DISCUSSION

A representation of the experimental workflow is depicted in Scheme 1. In this work, round Thermanox polymeric coverslips

were chosen as the substrate for surface grafting. Since these substrates are flexible, can be cut with scissors, and are designed to fit into the bottoms of a 24 well microtiter plate, gradient polymer coatings attached to them have many advantages for the future investigation of biological responses.³⁶ First, coverslips were coated with a 7.7 nm thick ethanol plasma coating, and then gradient plasma copolymerization of ethanol and ethyl 2-bromoisobutyrate (EBiB) formed a chemical gradient of ATRP initiators against this neutral background. Subsequently, DMA and PEGMA were polymerized from the surface initiators (Scheme 1).

Characterization of the Plasma Polymer Gradient.

Plasma polymerized samples derived from concurrent copolymerization of ethanol and EBiB were analyzed using ellipsometry and XPS. Figure 1 shows that the surface concentration of bromine (expressed as the Br/C ratio from XPS survey spectra) increases along the gradient. The Br/C content was observed to increase from nearly zero to 0.08 across the sample. A small but measurable quantity of bromine was detected on the surface during plasma polymerization of 100% ethanol vapor (i.e., at small values shown on the x -axis), which was not unexpected. When using a moving mask polymerization, it is not unknown that organic vapors in the plasma phase can diffuse and polymerize on areas of the samples not directly under the opening.³⁹ The maximal value of 0.08 is about half of the theoretically expected value of 0.167 for a pure, nonfragmented EBiB coating. The elemental composition of oxygen was also deficient by the same fraction suggesting that labile groups such as bromine and oxygen were lost in fragmentation/recombination reactions induced by the plasma and not deposited onto the surface.

High resolution C 1s XPS spectra were also obtained at all positions across the initiator gradient. One would expect that plasma copolymerization of two monomers simultaneously would result in surface spectra composed of contributions from both EBiB and ethanol plasma polymers in different proportions. Analysis positions on either end of the substrate correspond to mostly ethanol plasma polymer and mostly EBiB

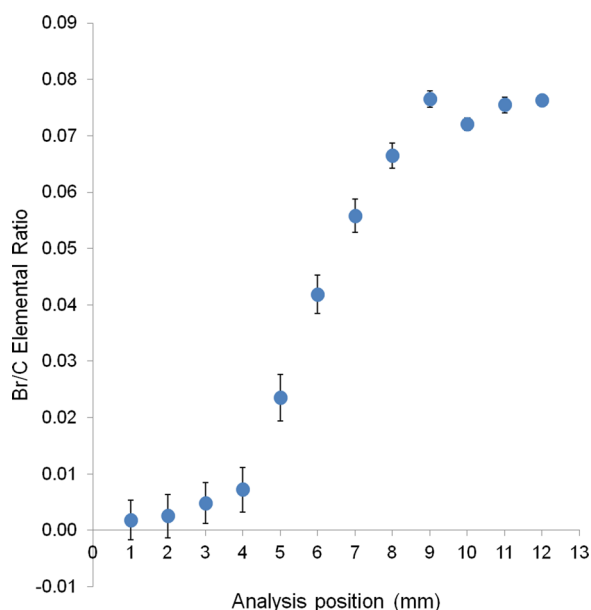


Figure 1. Quantification of Br/C elemental ratio determined by XPS at different positions along the surface of deposited ethanol/EBiB plasma copolymer.

plasma polymer respectively and peak fitting was used to confirm that the expected chemical environments were present (Figure 2a and b, respectively). We have studied ethanol plasma polymer before in both gradient copolymerizations¹⁵ and homopolymerizations.^{40,41} Qualitatively, the spectrum in Figure 2a contains the expected binding energy shifts and C 1s component proportions that correspond to the types of carbon–oxygen bonding environments for ethanol plasma polymer. We speculate that the C3 component is largely representative of hydroxyls bound to carbon atoms with, possibly, some contributions from ether environments as well.⁴⁰ The spectrum in Figure 2b is largely plasma polymer derived from EBiB; however, there will also be a small contribution from ethanol plasma polymer. Analysis of peak fitting suggests the presence of ester functionality as well as a component (C4) centered around 287.3 eV. Components C3 and C5 can reliably be assigned to $\text{C}-\text{O}$ and $\text{O}-\text{C}=\text{O}$, respectively. Components C3–C5 all have roughly the same area each making up 6–8% of the total C 1s peak area; thus, C4 would likely

correspond to the carbon bearing the dimethyl and bromine substituents positioned α to the carbonyl (i.e., $(\text{CH}_3)_2-\text{C}(\text{C}=\text{O})-\text{Br}$). Support for this assignment is derived from observation that the peak area corresponds roughly to the atomic percent of bromine in the survey spectrum (6 at. %). Further analysis of the high resolution Br 3d peak is presented in the Supporting Information (Figure S-1).

The use of ethanol plasma polymer in a counter gradient to EBiB helps to even out the thickness of the combined layer; otherwise, the thickness would have increased in a gradient fashion as well. The thickness profile of the plasma copolymer gradient by ellipsometry is shown in the Supporting Information (Figure S-2). Furthermore, use of ethanol as an inert “diluent” molecule provides nonreactivity and prevents against protein fouling, as we have shown previously.⁴⁰

The initiator plasma–polymer was stable and remained permanently adhered to the substrate for the duration of our experiments and analyses. Functionalized coverslips were soaked in the solvents used for polymerization (either water or 70 v/v% ethanol in water) for the same duration as the ATRP reaction (24 h) and were found to be stable with a similar and uniform thickness and surface chemical composition, which was comparable to nonsoaked samples.

Characterization of the Surface-Initiated Grafted Polymer Gradient. Coverslips functionalized with ethanol/EBiB plasma copolymer gradients were exposed to catalyst, ligand, and two different monomers for SI-ATRP. Reactions were carried out under aqueous⁶ or aqueous/alcohol²⁵ solvent conditions, as done previously. Evidence of successful grafting reactions was demonstrated by ellipsometry and XPS analysis.

After grafting with DMA, the thickness profile of the polymer layer at different positions across the gradient was obtained using ellipsometry (Figure 3). Additionally, the concentration of DMA was increased to produce polymer chains of increasing length resulting in a series of increasing graft thicknesses. Values reported are net polymer thicknesses obtained after subtraction of the initiator plasma polymer layer thickness. When probed across the sample from low initiator density to high initiator density, the thickness profile increased in a sigmoidal fashion matching the profile of bromine concentration (Figure 1). We discuss experimental reasons why the thickness data goes through a maximum and then decreases below.

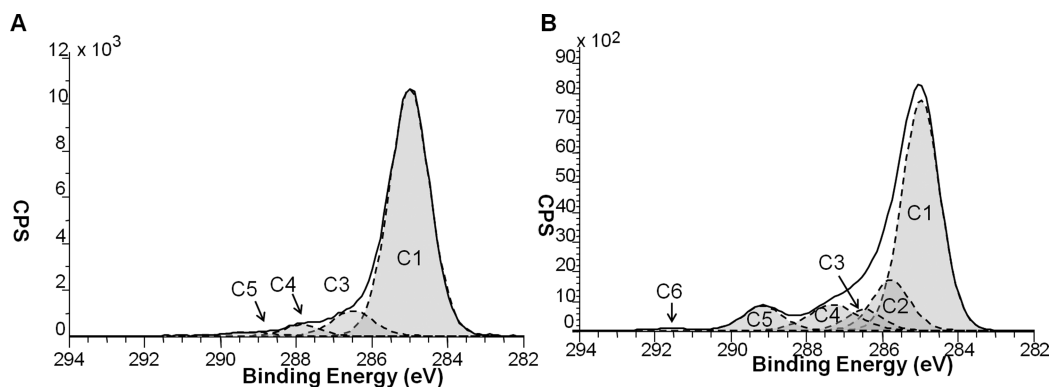


Figure 2. High resolution C 1s spectra at two positions along the initiator plasma copolymer gradient. (A) At the 1 mm position corresponding to the greatest proportion of ethanol plasma polymer. The peak was fit using 4 components and the C2 component was not identifiable owing to an absence of secondary-shifted peaks. (B) At the 12 mm position corresponding to the greatest proportion of EBiB plasma polymer. The peak was fit using 6 components. Definition of peak fitting components is given in the Materials and Methods section.

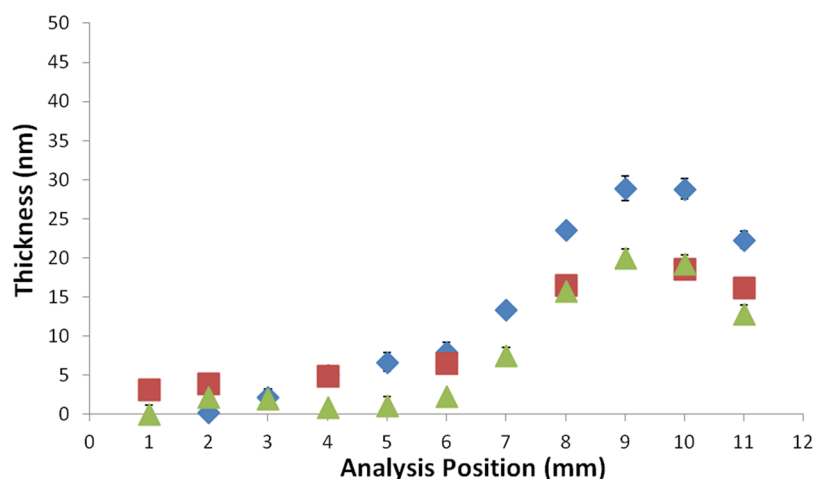


Figure 3. Grafted layer thickness of pDMA polymers as determined by ellipsometry at three monomer concentrations. \blacktriangle [DMA] = 0.10 M; \blacksquare [DMA] = 0.25 M; \blacklozenge [DMA] = 0.50 M. Values are expressed relative to the thickness of the initiator polymer layer.

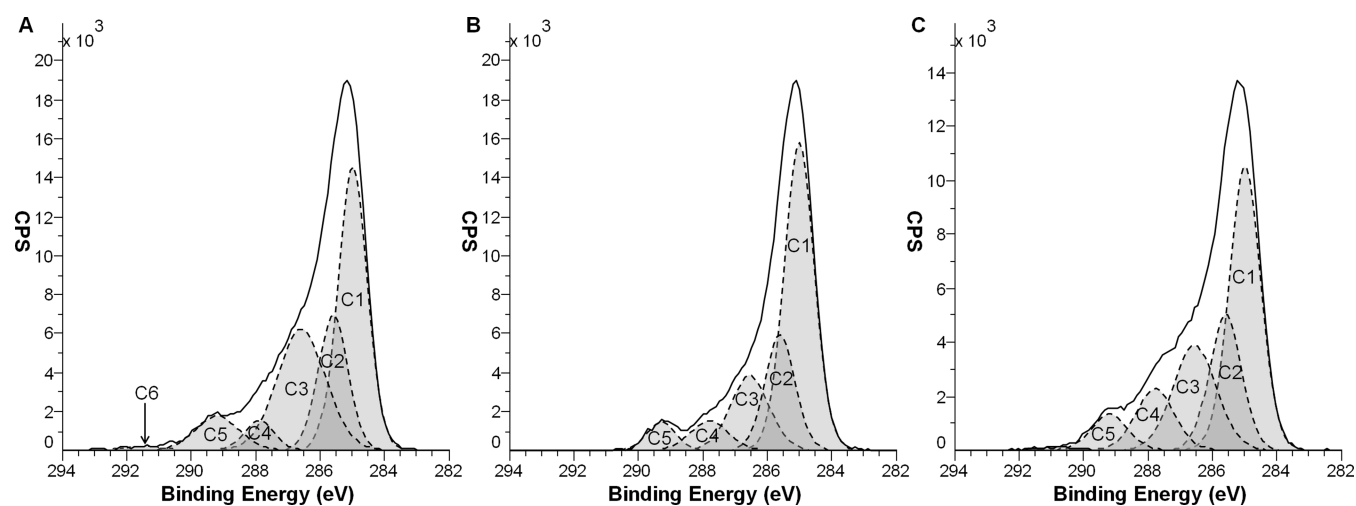


Figure 4. C 1s spectra for SI-ATRP grafted pDMA on EBiB/ethanol gradients. Monomer feed concentrations were (A) 0.10 M, (B) 0.25 M, (C) 0.50 M. In each case, the spectra were taken from analysis positions representative of the thickest polymer layer.

It could be argued that increased film thickness across the sample might be due to an increase in chain molecular weight (M_n) across the sample. However, on homogeneous surfaces, it is known that for low graft density samples, the rate of polymerization is faster than for high graft density samples.⁴² The physical result is that chains grafted from low density environments have larger M_n values under identical reaction conditions and time compared to high.^{43,44} Although the dependence of M_n on graft density is somewhat system dependent, it is shown to be quite strong for low density surfaces, becoming weaker and nearly independent when the fractional initiator content is greater than 10–40%.⁴² Thus, a likely view of our gradient grafted surfaces (where we have provided sufficient mixing of ATRP reactants) would be that chains would be relatively longer at low sample positions (low initiator densities) becoming shorter and have nearly identical M_n values from the midpoint of the gradient onward. This provides a convincing view that surface crowding is responsible for the dramatic increase in dry thickness across the gradient. On the low density side, longer chains adopt a mushroom (or in air, collapsed) conformation and contribute minimally to the dry thickness increase seen to be less than 5 nm. As the grafting density increased, due to entropic penalties, chains would be

forced to stretch away from the surface in a brush morphology to access free volume above the interface. This produces a much greater observed dry thickness that is on the order of tens of nanometers. The increased thickness on the high density side would be despite having likely shorter chains compared to the low density side. This view of the energetic properties of grafted polymer gradient surfaces and the observed sigmoidal thickness profile is consistent with the works of others.^{17,45}

Qualitatively, the high resolution C 1s profiles obtained were characteristic for carbon bonding environments for amide-containing polymers (e.g., polyacrylamides) (Figure 4). With increasing [DMA], the C 1s spectra showed increased acrylamide character via the greater proportion of the C4 component. These spectra were comparable to spectra typical of grafted pDMA.²⁶ Along the gradient, XPS analysis of regions showed increasing acrylamide character (SI Figure S-3) as the polymer layer thickness increased and the contribution to the XPS signal from the underlying EBiB/ethanol plasma polymer substrate was reduced accordingly.

Surface grafting was also carried out using PEGMA—a methacrylate-based monomer bearing a short oligo-PEG chain. Compared with DMA, ellipsometry revealed that, in general, much thicker polymer graft layers were obtained. Furthermore,

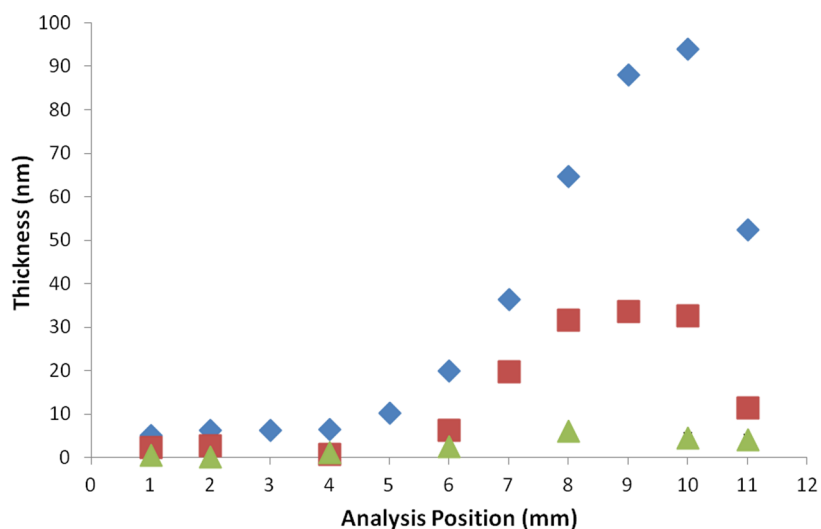


Figure 5. Grafted layer thickness of pPEGMA polymers as determined by ellipsometry at three monomer concentrations. \blacktriangle [PEGMA] = 0.20 M; \blacksquare [PEGMA] = 0.50 M; \blacklozenge [PEGMA] = 1.0 M. Values are expressed relative to the thickness of the initiator polymer layer.

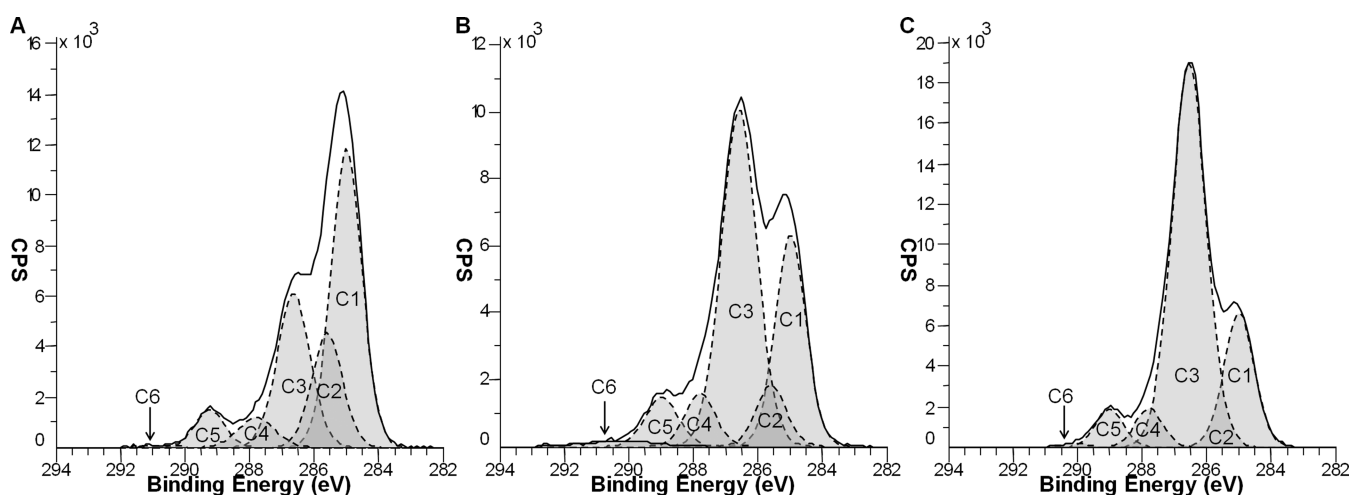


Figure 6. C 1s spectra for SI-ATRP grafted pPEGMA475 on EBiB/ethanol gradients. Monomer feed concentrations were (A) 0.2 M, (B) 0.5 M, (C) 1.0 M. In each case, the spectra were taken from analysis positions representative of the thickest polymer layer.

the variation in the coating thickness on the low-graft density side and the high-graft density side was much greater. The maximum dry pPEGMA grafted layer thicknesses increased from 5 to 34 nm for 0.2 and 0.5 M, respectively, and to 94 nm (maximum) for 1 M (Figure 5). Scattered light from these thickest-grafted samples could be seen by the naked eye as a gradient increase in cloudiness across the coverslip. The direction of the increasing cloudiness corresponded to the markings indicating the direction of increasing surface initiator content.

Qualitatively, the high resolution C 1s profiles show carbon bonding environments characteristic for PEG-like polymers (Figure 6), that is, a high proportion of C3 component, which corresponds to the C—O present in ethers such as PEG. Similar to results above, with increasing [PEGMA] thicker layers resulted giving stronger indications of ether photoelectrons. XPS analysis locations along the gradient demonstrated a similar trend in increasing C—O—C character across the sample (SI, Figure S-4) with spectra and peak fittings resembling those observed previously.²⁵ Again, increasing polymer layer thickness is consistent with the view that

entropic effects result from increased polymer stretching caused by closer and closer grafting densities across the sample.

Data for both pDMA and pPEGMA gradients, showed the thickness profile going through a maximum and then decreasing near the end of maximum-EBiB side of the substrate. There are a few possible explanations for this observation. First, both ellipsometry and XPS use relatively wide beams of energy compared to the gradient length scale in this experiment. The X-ray beam approaches 1 mm wide, and the beam of light in ellipsometry can stretch to several mm wide as the angle of incidence is lowered. When probing an estimated 1 mm from the sample edge, signal is scattered from the edge, and a substantial portion of the signal can be lost as wide beams are not reflected from the substrate. Second, there may be inhomogeneities in the plasma polymer near the substrate edge due to diffusion of the plasma polymer under the mask, as mentioned above. We note a couple of other reports that showed similar maxima and dips near the substrate edge for different plasma polymer systems.^{36,39}

Using our straightforward procedure, we have shown that changing the initiator surface density and also the graft length

(through increasing monomer concentration) resulted in film thickness changes arising from chain stretching—a well understood consequence of the system entropy.^{3,8,10,15,45} While the changes in film thickness due to increased surface crowding (density) were readily apparent from Figures 3 and 5, it is worth briefly commenting on differential observed thickness changes resulting from linear and bottle-brush polymers. Intuitively, increasing the monomer concentration causes thickness increases for both pDMA and pPEGMA simply because the degree of polymerization is greater and chains are longer. However, with DMA as the monomer, and the monomer feed concentration doubled, the observed dry layer thickness for linear polymers increased by a maximum of 1.4 times. This is less than the theoretical value of 2 probably resulting from thickness determinations being performed in the polymer-collapsed dry state on a variable graft density surface. With a bulky monomer such as PEGMA in which each methacrylate repeat unit bears an oligo-PEG polymer chain, the relative thickness increase was much greater. Here, doubling the monomer concentration produced a maximum dry layer thickness change of 2.9 times. This larger thickness change confirms that the bulkier bottle-brush polymers give rise to an increased number of interchain contacts, which shows the entropic contribution to chain stretching based on degree of polymerization—much more so than for linear polymers.

It is well-known that the entropic properties of grafted polymer surfaces are important in protein adsorption with relationships to both graft density and graft length.^{3,10,28,45} We believe our system would be well-suited to investigations of interfacial properties of polymer brush systems and provides an advantage over multistep gradient fabrication methods. Also, since the method is substrate independent, there is outstanding versatility in being able to fabricate grafted surfaces for biological studies on different materials such as glass, plastic, or even metal surfaces for sensing applications.

CONCLUSIONS

Plasma polymerization of ethyl 2-bromoisobutyrate has been described for the first time. When coated on surfaces by plasma polymer thin film deposition, the retained reactivity of the halogen species allowed successful SI-ATRP to be performed. Surfaces bearing carbonyls with 2-bromoisobutyrate substituents are a commonly reported pathway to preparing grafted surfaces; however, these initiator residues have never been described before in a procedure that allows for one step substrate independent functionalization. Further, we have shown that the surface density of initiators could be controlled across the substrate. Polymer brushes grafted from this gradient surface resulted in large thickness differences across the sample due to chain stretching. The response in chain stretching was clearly a function of the entropy of the system with linear pDMA polymers having a lower degree of stretching compared to “bottle-brush” pPEGMA polymers.

ASSOCIATED CONTENT

Supporting Information

Overlay of Br 3d high resolution XPS spectra at different positions along the gradient. Thickness of the initiator plasma polymer determined by ellipsometry. Overlay of C 1s high resolution XPS spectra for pDMA and pPEGMA polymer coatings at different positions along the gradient. This material is available free of charge via the Internet at <http://pubs.acs.org/>.

AUTHOR INFORMATION

Corresponding Author

*Email: bryan.coad@unisa.edu.au

Notes

The authors declare no competing financial interest.

REFERENCES

- (1) Fristrup, C. J.; Jankova, K.; Hvilsted, S. Surface-Initiated Atom Transfer Radical Polymerization—A Technique to Develop Biofunctional Coatings. *Soft Matter* **2009**, *5*, 4623–4634.
- (2) Xu, F. J.; Neoh, K. G.; Kang, E. T. Bioactive Surfaces and Biomaterials via Atom Transfer Radical Polymerization. *Prog. Polym. Sci.* **2009**, *34*, 719–761.
- (3) Feng, W.; Brash, J. L.; Zhu, S. P. Non-biofouling Materials Prepared by Atom Transfer Radical Polymerization Grafting of 2-Methacryloxyethyl Phosphorylcholine: Separate Effects of Graft Density and Chain Length on Protein Repulsion. *Biomaterials* **2006**, *27*, 847–855.
- (4) Barbey, R.; Lavanant, L.; Paripovic, D.; Schüwer, N.; Sugnaux, C.; Tugulu, S.; Klok, H.-A. Polymer Brushes via Surface-Initiated Controlled Radical Polymerization: Synthesis, Characterization, Properties, and Applications. *Chem. Rev.* **2009**, *109*, 5437–5527.
- (5) Edmondson, S.; Osborne, V. L.; Huck, W. T. S. Polymer Brushes via Surface-Initiated Polymerizations. *Chem. Soc. Rev.* **2004**, *33*, 14–22.
- (6) Coad, B. R.; Kizhakkedathu, J. N.; Haynes, C. A.; Brooks, D. E. Synthesis of Novel Size Exclusion Chromatography Support by Surface Initiated Aqueous Atom Transfer Radical Polymerization. *Langmuir* **2007**, *23*, 11791–11803.
- (7) de Gennes, P. G. Conformations of Polymers Attached to an Interface. *Macromolecules* **1980**, *13*, 1069–1075.
- (8) Milner, S. T. Polymer Brushes. *Science* **1991**, *251*, 905–914.
- (9) Zhang, Z.; Chen, S. F.; Chang, Y.; Jiang, S. Y. Surface Grafted Sulfobetaine Polymers via Atom Transfer Radical Polymerization as Superlow Fouling Coatings. *J. Phys. Chem. B* **2006**, *110*, 10799–10804.
- (10) Ma, H. W.; Wells, M.; Beebe, T. P.; Chilkoti, A. Surface-Initiated Atom Transfer Radical Polymerization of Oligo(ethylene glycol) Methyl Methacrylate from a Mixed Self-Assembled Monolayer on Gold. *Adv. Funct. Mater.* **2006**, *16*, 640–648.
- (11) Genzer, J. Templating Surfaces with Gradient Assemblies. *J. Adhes.* **2005**, *81*, 417–435.
- (12) Bhat, R. R.; Tomlinson, M. R.; Wu, T.; Genzer, J. Surface-Grafted Polymer Gradients: Formation, Characterization, and Applications. *Adv. Polym. Sci.* **2006**, *198*, 51–124.
- (13) Genzer, J.; Bhat, R. R. Surface-Bound Soft Matter Gradients. *Langmuir* **2008**, *24*, 2294–2317.
- (14) Kim, M. S.; Khang, G.; Lee, H. B. Gradient Polymer Surfaces for Biomedical Applications. *Prog. Polym. Sci.* **2008**, *33*, 138–164.
- (15) Wu, T.; Efimenko, K.; Genzer, J. Combinatorial Study of the Mushroom-to-Brush Crossover in Surface Anchored Polyacrylamide. *J. Am. Chem. Soc.* **2002**, *124*, 9394–9395.
- (16) Wu, T.; Genzer, J.; Gong, P.; Szeleifer, I.; Vlček, P.; Šubr, V. In *Polymer Brushes: Synthesis, Characterization, Applications*; Advincula, R. C.; Brittain, W. J.; Caster, K. C.; Rühle, J., Eds.; Wiley-VCH Verlag GmbH & Co. KGaA: Weinheim, 2004; Chapter 15, pp 287–315.
- (17) Wang, X.; Tu, H.; Braun, P. V.; Bohn, P. W. Length Scale Heterogeneity in Lateral Gradients of Poly(N-isopropylacrylamide) Polymer Brushes Prepared by Surface-Initiated Atom Transfer Radical Polymerization Coupled with In-Plane Electrochemical Potential Gradients. *Langmuir* **2006**, *22*, 817–823.
- (18) Yasuda, H. In *New Methods of Polymer Synthesis*; Ebdon, J. R.; Eastmond, G. C., Eds.; Blackie Academic & Professional: London, 1995; Chapter 5, pp 161–196.
- (19) Chan, C. M.; Ko, T. M.; Hiraoka, H. Polymer Surface Modification by Plasmas and Photons. *Surf. Sci. Rep.* **1996**, *24*, 3–54.
- (20) Siow, K. S.; Britcher, L.; Kumar, S.; Griesser, H. J. Plasma Methods for the Generation of Chemically Reactive Surfaces for Biomolecule Immobilization and Cell Colonization—A Review. *Plasma Processes Polym.* **2006**, *3*, 392–418.

- (21) Coad, B. R.; Jasieniak, M.; Griesser, S. S.; Griesser, H. J. Controlled Covalent Surface Immobilisation of Proteins and Peptides Using Plasma Methods. *Surf. Coat. Technol.* **2013**, *233*, 169–177.
- (22) Vasilev, K.; Michelmor, A.; Griesser, H. J.; Short, R. D. Substrate Influence on the Initial Growth Phase of Plasma-Deposited Polymer Films. *Chem. Commun.* **2009**, 3600–3602.
- (23) Chen, R. T.; Muir, B. W.; Thomsen, L.; Tadich, A.; Cowie, B. C. C.; Such, G. K.; Postma, A.; McLean, K. M.; Caruso, F. New Insights into the Substrate–Plasma Polymer Interface. *J. Phys. Chem. B* **2011**, *115*, 6495–6502.
- (24) Yameen, B.; Khan, H. U.; Knoll, W.; Förch, R.; Jonas, U. Surface Initiated Polymerization on Pulsed Plasma Deposited Polyallylamine: A Polymer Substrate-Independent Strategy to Soft Surfaces with Polymer Brushes. *Macromol. Rapid Commun.* **2011**, *32*, 1735–1740.
- (25) Coad, B. R.; Lu, Y.; Glattauer, V.; Meagher, L. A Substrate Independent Method for Growing and Modulating the Density of Polymer Brushes from Surfaces by ATRP. *ACS Appl. Mater. Interfaces* **2012**, *4*, 2811–2823.
- (26) Coad, B. R.; Lu, Y.; Meagher, L. A Substrate-Independent Method for Surface Grafting Polymer Layers by Atom Transfer Radical Polymerization: Reduction of Protein Adsorption. *Acta Biomater.* **2012**, *8*, 608–618.
- (27) Coad, B. R.; Bilgic, T.; Klok, H.-A. Polymer Brush Gradients Grafted from Plasma-Polymerized Surfaces. *Langmuir* **2014**, Under review.
- (28) Tugulu, S.; Klok, H.-A. Stability and Nonfouling Properties of Poly(poly(ethylene glycol) methacrylate) Brushes-under Cell Culture Conditions. *Biomacromolecules* **2008**, *9*, 906–912.
- (29) Teare, D. O. H.; Barwick, D. C.; Schofield, W. C. E.; Garrod, R. P.; Ward, L. J.; Badyal, J. P. S. Substrate-Independent Approach for Polymer Brush Growth by Surface Atom Transfer Radical Polymerization. *Langmuir* **2005**, *21*, 11425–11430.
- (30) Morsch, S.; Schofield, W. C. E.; Badyal, J. P. S. Surface Actuation of Smart Nanoshutters. *Langmuir* **2010**, *26*, 12342–12350.
- (31) Morsch, S.; Schofield, W. C. E.; Badyal, J. P. S. Tailoring the Density of Surface-Tethered Bottlebrushes. *Langmuir* **2011**, *27*, 14151–14159.
- (32) Morsch, S.; Wood, T. J.; Schofield, W. C. E.; Badyal, J. P. S. A Combined Plasmachemical and Emulsion Templating Approach for Actuated Macroporous Scaffolds. *Adv. Funct. Mater.* **2012**, *22*, 313–322.
- (33) Schofield, W. C. E.; Bain, C. D.; Badyal, J. P. S. Cyclodextrin-Functionalized Hierarchical Porous Architectures for High-Throughput Capture and Release of Organic Pollutants from Wastewater. *Chem. Mater.* **2012**, *24*, 1645–1653.
- (34) Matyjaszewski, K.; Wang, J.-L.; Grimaud, T.; Shipp, D. A. Controlled/"Living" Atom Transfer Radical Polymerization of Methyl Methacrylate Using Various Initiation Systems. *Macromolecules* **1998**, *31*, 1527–1534.
- (35) Whittle, J. D.; Barton, D.; Alexander, M. R.; Short, R. D. A Method for the Deposition of Controllable Chemical Gradients. *Chem. Commun.* **2003**, 1766–1767.
- (36) Robinson, D. E.; Marson, A.; Short, R. D.; Buttle, D. J.; Day, A. J.; Parry, K. L.; Wiles, M.; Highfield, P.; Mistry, A.; Whittle, J. D. Surface Gradient of Functional Heparin. *Adv. Mater.* **2008**, *20*, 1166–1169.
- (37) Goreham, R. V.; Short, R. D.; Vasilev, K. Method for the Generation of Surface-Bound Nanoparticle Density Gradients. *J. Phys. Chem. C* **2011**, *115*, 3429–3433.
- (38) Gengenbach, T. R.; Chatelier, R. C.; Griesser, H. J. Characterization of the Ageing of Plasma-Deposited Polymer Films: Global Analysis of X-ray Photoelectron Spectroscopy Data. *Surf. Interface Anal.* **1996**, *24*, 271–281.
- (39) Vasilev, K.; Mierczynska, A.; Hook, A. L.; Chan, J.; Voelcker, N. H.; Short, R. D. Creating Gradients of Two Proteins by Differential Passive Adsorption onto a PEG-Density Gradient. *Biomaterials* **2010**, *31*, 392–397.
- (40) Coad, B. R.; Vasilev, K.; Diener, K. R.; Hayball, J. D.; Short, R. D.; Griesser, H. J. Immobilized Streptavidin Gradients as Bioconjugation Platforms. *Langmuir* **2012**, *28*, 2710–2717.
- (41) Coad, B. R.; Scholz, T.; Vasilev, K.; Hayball, J. D.; Short, R. D.; Griesser, H. J. Functionality of Proteins Bound to Plasma Polymer Surfaces. *ACS Appl. Mater. Interfaces* **2012**, *4*, 2455–2463.
- (42) Bao, Z.; Bruening, M. L.; Baker, G. L. Control of the Density of Polymer Brushes Prepared by Surface-Initiated Atom Transfer Radical Polymerization. *Macromolecules* **2006**, *39*, 5251–5258.
- (43) Jones, D. M.; Brown, A. A.; Huck, W. T. S. Surface-Initiated Polymerizations in Aqueous Media: Effect of Initiator Density. *Langmuir* **2002**, *18*, 1265–1269.
- (44) Nagase, K.; Kobayashi, J.; Kikuchi, A. I.; Akiyama, Y.; Kanazawa, H.; Okano, T. Effects of Graft Densities and Chain Lengths on Separation of Bioactive Compounds by Nanolayered Thermoresponsive Polymer Brush Surfaces. *Langmuir* **2008**, *24*, 511–517.
- (45) Wu, T.; Efimenko, K.; Vlcek, P.; Subr, V.; Genzer, J. Formation and Properties of Anchored Polymers with a Gradual Variation of Grafting Densities on Flat Substrates. *Macromolecules* **2003**, *36*, 2448–2453.